Photochemical fabrication of three-dimensional micro- and nano-structured surfaces from a C_{60} monoadduct

Parvez Iqbal,[a] Shuqing Sun,[b] Marcus D. Hanwell,[c] David Attwood,[d] Graham J. Leggett,*[b] Jon A. Preece,*[a] Tim H. Richardson[c] and David Tunnicliffe[d]

Received 7th December 2007, Accepted 21st February 2008
First published as an Advance Article on the web 6th March 2008
DOI: 10.1039/b718888a

Exposure of Langmuir–Blodgett (LB) films of a C_{60} adduct supported on silicon wafers to UV light leads to cross-linking of the C_{60} moieties, which are resistant to removal by solvent exposure, whereas unexposed moieties are readily removed. This process provides a convenient and simple route for the fabrication of highly conjugated surface-attached structures, with dimensions ranging from micrometres (using masks) to a few tens of nanometres using light emitted from a scanning near-field optical microscope (SNOM). The SNOM writing velocity was found to significantly affect the lateral resolution and the height of the three-dimensional nanostructures. Increasing the writing velocity from 0.3 to 2 μm s^{-1} resulted in a decrease in the width of the structures from 240 nm to 70 nm (corresponding to the SNOM aperture diameter), respectively, and a reduction in the height from 8 nm (the thickness of the original film) to 3 nm, respectively. This approach provides a simple, direct route to surface-bound nanometre scale assemblies of C_{60}.

1 Introduction

Light is an attractive tool for the fabrication of structures and devices because of the paradigmatic status of photolithography in semiconductor device fabrication and the availability of a large toolkit of synthetic photochemical methodologies. The principal problem associated with the application of photochemical methods of fabrication has previously been thought to be the dominance of the diffraction effects as the Rayleigh limit is approached. Recently, however, the application of novel optical phenomena has opened up exciting prospects for photochemical modification of materials with a resolution significantly superior to that of conventional approaches. These include the exploitation of interferometric methods[1–3] and of plasmonic phenomena,[4–7] which are currently attracting rapidly growing interest.

One successful approach to the fabrication of nanostructures has been the exploitation of the near-field optical methods. Using a scanning near-field optical microscope (SNOM) coupled to a UV laser, self-assembled monolayers have been patterned and used as templates for the etching of structures in gold films with a resolution that may be as good as 9 nm, nearly $\lambda/30$.[8–12] This approach, which we have termed scanning near-field photolithography (SNP) provides a significant advance in photolithographic capability. Previously, however, it has predominantly been applied to the patterning of alkanethiol systems. Recently we have begun to explore its application to other types of photoactive materials, including monolayers of alkylsilanes.[13] Recently, we reported a simple route to the fabrication of metal nanowires by utilizing near-field exposure of gold nanoparticles.[14] Langmuir–Schaeffer films (bilayers) of thiol-stabilized gold nanoparticles were formed on silicon substrates and selectively exposed to UV light from a near-field probe. The result was the coagulation of the nanoparticles to form wires *ca.* 60 nm in width. Here we report a new route to the fabrication of C_{60} structures that utilises a similar simple methodology. Synthetic modification of the C_{60} molecules renders them readily amenable to Langmuir–Blodgett film formation[15] and the photochemical cross-linking yields robust structures in a single step.

Since C_{60}, or buckminsterfullerene, was first discovered by Kroto *et al.*[16] in 1985, fullerenes have received a great deal of attention because of the unique properties of their extended π-systems, giving rise to potential applications in the biological,[17] electrical[18] and chemical[19] sciences. In 1991, Rao *et al.*[20] reported for the first time that C_{60} was photosensitive. It was observed that after exposure to UV light, a C_{60} film became insoluble in toluene. Evidence from laser desorption mass spectroscopy, infrared spectroscopy, Raman spectroscopy and optical absorption spectroscopy gave strong indications that the C_{60} had polymerised and the C_{60} clusters had not been destroyed during the UV light exposure. In addition, X-ray diffraction showed that the films became more disordered after the UV light exposure and the lattice had contracted. Initially, it was thought[20] that a 2πs + 2πs photochemical cycloaddition reaction was causing the cross-linking. However, the contraction seen between neighbouring C_{60} molecules was smaller than expected, and it was then proposed[20] that an =C=C= allene-type bridge may have been formed between the C_{60} moieties to form C_{60}=C=C=C_{58}. After further spectroscopic studies

[a]*School of Chemistry, University of Birmingham, Edgbaston, Birmingham, UK, B15 2TT*
[b]*Department of Chemistry, University of Sheffield, Brook Hill, Sheffield, UK, S3 7HF*
[c]*Department of Physics and Astronomy, University of Sheffield, Hounsfield Road, Sheffield, UK, S3 7RH*
[d]*BAE SYSTEMS Advanced Technology Centre, PO Box 5, Filton, Bristol, UK, BS34 7QW*

performed by members of the same group[21] and theoretical calculations made by Menon *et al.*,[22] the formation of the allene-type bridge was ruled out and 2πs + 2πs photochemical cycloaddition was proposed as the most likely mechanism, whereby two σ-bonds are formed between two adjacent C_{60} cages leading to the formation of a 4-membered ring. Later experimental studies[23–25] and theoretical calculations[24,26,27] concur with the mechanism being 2πs + 2πs photochemical cycloaddition. The polymerisation is thought to be initiated by the dimerisation between two adjacent C_{60} cages followed by further 2πs + 2πs cycloadditions to form longer oligomers.[24,25] Often, it has been observed that there are a number of oligmers formed with the dimer being the most abundant.[20,24,27] The distribution of the oligomers formed is affected by temperature at which the polymerisation is performed.[24,25]

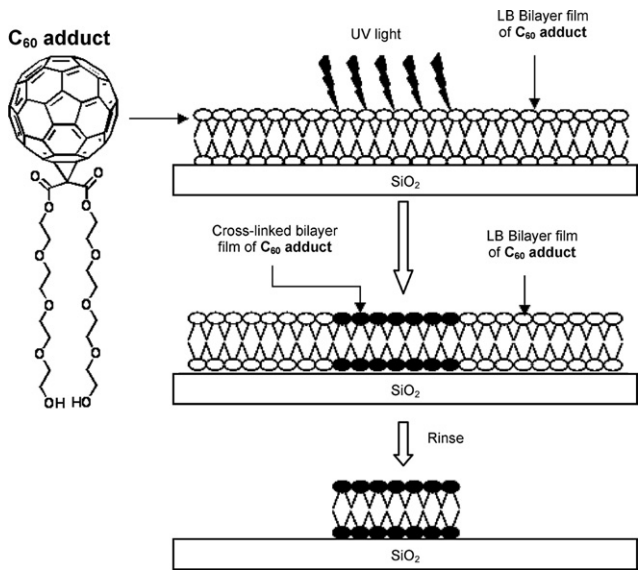

Fig. 1 The C_{60} adduct and a schematic diagram (right) showing the patterning methodology.

The effect of electron beam irradiation on C_{60} is remarkably different. Although electron beam irradiation renders C_{60} and its methanofullerene derivatives insoluble in toluene compared to unirradiated regions,[28–32] it is also well documented that the electron beam irradiation leads to extensive cage fragmentation and the formation of disordered networks of graphite-like particles.[30] In fact, the methanofullerene derivatives have been shown to have potential as negative tone resists for electron beam lithography and they are achieving better sensitivity than some of the commercially available polymers such as poly(methyl-methacrylate) (PMMA).[32]

The clear advantage of a photolithographic patterning process would thus be that it offers the possibility of cross-linking C_{60} while causing minimal modification to its molecular structure. The drawback has previously been the limited resolution associated with photopatterning techniques. Here we demonstrate that by using near-field methods it is possible to realise exceptional resolution during the photochemical fabrication of C_{60} nanostructures.

The process used in the present study is illustrated in Fig. 1. Langmuir films of the amphiphilic C_{60} adduct were transferred on to the Si/SiO_2 substrate *via* the Langmuir–Blodgett (LB) technique, followed by irradiation with UV light (244 nm) either in a parallel fashion through a mask or serially with the SNOM. The irradiation induces the cross-linking in the C_{60} moieties rendering the irradiated areas insoluble, such that the unirradiated areas of the C_{60} adduct film may easily be removed by rinsing with chloroform leaving the insoluble irradiated C_{60} film intact.

2 Results and discussions

The synthesis of the C_{60} adduct is shown in Scheme 1. The derivatisation was achieved by the reaction of 3,4-dihydro-3′*H*-pyran (THP) with tetraethylene glycol (**1**) in the presence of

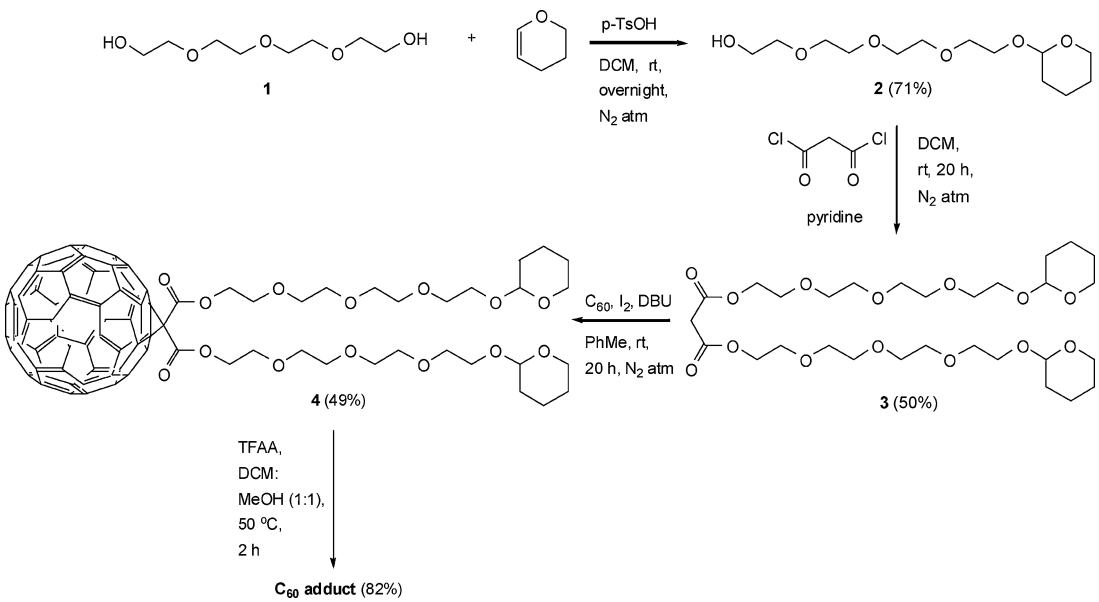

Scheme 1 Synthesis of the C_{60} adduct.

p-toluenesulfonic acid monohydrate. The resultant monosubstituted tetrahydropyranyl ethylene glycol (**2**) was esterified with malonyl dichloride in the presence of pyridine, affording the bis-ester (**3**). The cyclopropyl fullerene bis-ester (**4**) was synthesized *via* the Bingel reaction[33] between the bis-ester (**3**) and C_{60} in the presence of base and iodine in the dark. The THP moieties were removed by TFAA to afford the C_{60} adduct.

The *Π–A* isotherms for the compression (10 cm^2 min^{-1}) and decompression (10 cm^2 min^{-1}) of the C_{60} adduct Langmuir film are shown in Fig. 2. Three cycles are shown. The liquid expanded phase (LE) in cycle 1 persists to just below 1 nm^2. This value is in good agreement with the molecular area of the C_{60} (0.75 nm^2). The surface pressure rises rapidly to ~20 mN m^{-1} at an area per molecule of 0.5 nm^2, at which point a kink in the curve appears. After the kink the rate of increase in surface pressure decreases, which suggests possible shearing of the film forming a partial bilayer. Decompression and recompression (cycles 2 and 3) reveal that the onset of pressure from the liquid expanded (LE) phase occurs at increasingly smaller areas per molecule indicating aggregation and/or bilayer structures.[34–36]

The C_{60} adduct Langmuir films were transferred to the substrate at a fixed surface pressure of 30 mN m^{-1}, and a dipping velocity of 5 mm min^{-1}. Samples were prepared by transferring two/three bilayers using Langmuir–Blodgett deposition techniques. The resulting film structures were characterised by tapping mode atomic force microscopy (AFM). A representative image is shown in Fig. 3a. The surface is uniformly covered with the C_{60} adduct, and there is no evidence of any defects. The topography of the films did not change over 3 days suggesting that they remained stable over this period. The thicknesses of the films were determined by measuring the step height between the covered and uncovered regions of the substrate, and were found to be 8 and 12 nm, which are consistent with two and three bilayers of the C_{60} adduct, respectively.

To investigate whether the C_{60} adduct films were photosensitive and stable after UV light irradiation, films consisting of three bilayers were exposed to UV light through a Cu TEM grid (λ = 244 nm) for 1 min. Fig. 3a shows an AFM image of the film before irradiation and Fig. 3b after irradiation. It is clear that there has been no change in the film topography. However, after rinsing with $CHCl_3$ the masked areas of the film were removed, while the film exposed to UV light remained on the surface (Fig. 3c). Well-defined square islands with lateral dimensions equal to the width of the mask features and a vertical dimension of ~12 nm were observed.

Nanoscale patterns were fabricated by exposing the films of the C_{60} adduct with UV light from a near-field probe. Two bilayers were deposited on a hydrophobic silicon substrate. After exposure, the films were rinsed with $CHCl_3$. Again, the resulting cross-linked structures were found to be stable, while the unexposed material was easily removed. A variety of writing rates were used to examine whether there was an influence on the resulting feature size. Fig. 4 shows the AFM images of the samples patterned at SNOM scan velocities of 0.3, 1 and 2 μm s^{-1}. All the images show that well-defined, continuous structures, which are free from defects, have been formed, with the line thickness varying with the writing rate. Lines formed with writing velocities of 0.3, 1 and 2 μm s^{-1} exhibited full widths at

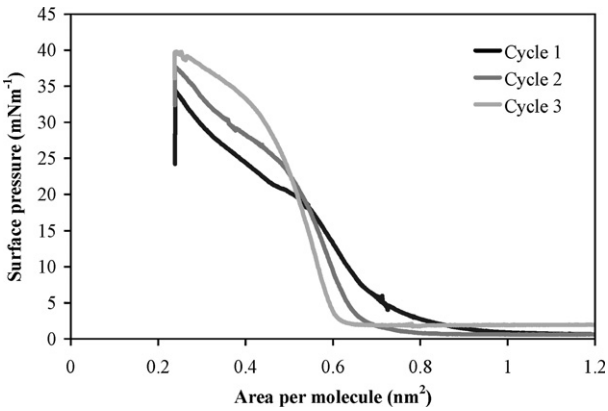

Fig. 2 *Π–A* Isotherm of the C_{60} adduct.

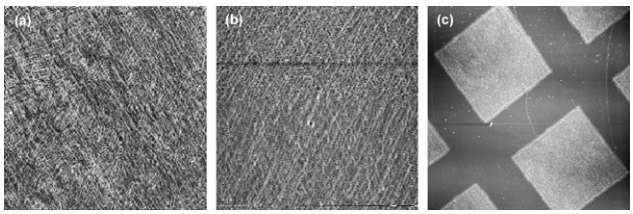

Fig. 3 AFM images of the C_{60} adduct films (a) before and (b) after exposure to UV light for 1 min, and (c) after rinsing with $CHCl_3$. Image sizes: (a), (b) are 20 × 20 $μm^2$, and (c) is 100 × 100 $μm^2$.

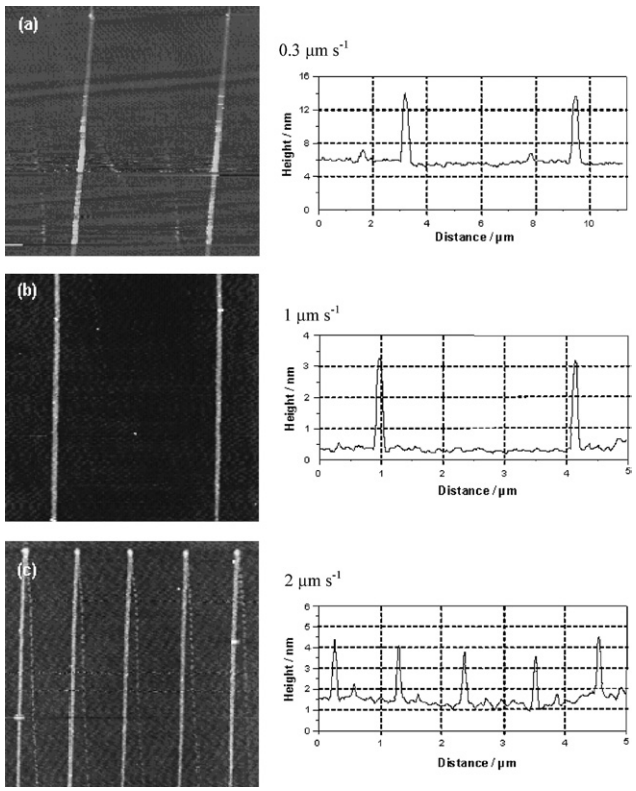

Fig. 4 Representative AFM images and cross-section analysis for the nanostructures formed after writing onto 2 bilayers of the C_{60} adduct LB films with SNOM writing velocities of (a) 0.3 μm s^{-1}, (b) 1 μm s^{-1}, (c) 2 μm s^{-1} and rinsing the films with $CHCl_3$.

half maximum height (FWHM) of ~240, ~100, ~70 nm, respectively. The line lateral thickness observed with writing velocity of 2 μm s^{-1} is comparative to the diameter of the aperture of the SNOM probe (~70 nm), and hence indicates that the polymerisation of the film has not spread outside the area illuminated by the probe, whereas, at the slower velocities, 0.3 and 1 μm s^{-1}, some polymerisation has extended laterally through the film. It is known that the electric field associated with a near-field excitation diverges reasonably rapidly through a dielectric medium, and the most likely explanation for the observation of structures larger than the aperture diameter here is the effective spreading of the excitation through the finite depth of the resist medium (*ca.* 8 nm for two bilayers of C_{60} adduct). Nevertheless, the resolutions exhibited by the structures in Fig. 4 are extremely good.

The height of the structures formed with writing velocity of 0.3, 1 and 2 μm s^{-1} are observed as ~8, ~3 and ~3 nm, respectively. The height of the structure obtained with writing velocity of 0.3 μm s^{-1} is comparable to the C_{60} adduct LB film (~8 nm, determined from AFM), whereas at the faster velocities the structures are less than half of the initial LB film thickness (before irradiation). This observation suggests that incomplete polymerisation occurs at faster writing times (*i.e.* lower dwell times), and the C_{60} adducts are not fully polymerised and may be rinsed away.

In some images, narrow, discontinuous lines may be observed that extend diagonally between the main features created lithographically. These are thought to be artifacts resulting from the minimal exposure of the samples as the probe moved rapidly (35 μm s^{-1}) from the end of one line to the beginning of the next structure to be written. It appears even at this much reduced exposure the C_{60} adduct film is still partially polymerised, leading to even thinner (but incomplete) lines.

3 Conclusion

In summary, it is clear that near-field optical methods provide a simple route to the fabrication of surface-bound nanostructures composed of C_{60} building blocks. This methodology may have widespread utility in the fabrication of functional molecular nanostructures. The relatively small perturbation of the molecular structure of the C_{60} moieties *via* (i) the attachment of the hydrophilic glycol chain in the formation of the C_{60} adduct, and (ii) the subsequent photochemical cross-linking in the LB films, coupled to the small inter C_{60} moiety separation in the nanowires lends itself to the exciting possibility that these nanowires may very well be electrically conductive as a result of overlap of the π-frameworks from neighbouring molecules. Currently we are examining this aspect further. The integration of novel nanolithographic methodologies that can induce specific chemical reactions in nanomaterials presents a new paradigm for the fabrication of nanostructured surfaces with three-dimensional form and potential function.

4 Experimental

4.1 Chemicals

Unless otherwise stated, all commercially available chemicals were purchased from Aldrich and were used as received. C_{60} was purchased from the Mer Corporation and was used as received. Solvents were either used as received or dried; DCM from CaH_2, THF and PhMe were distilled from Na–benzophenone ketyl under a N_2 atmosphere. Thin-layer chromatography (TLC) was carried out on aluminium plates coated with silica gel 60 F254 (Merck 5554). The TLC plates were air-dried and analysed under a short wave UV lamp (254 nm) or by developing the TLC plates in an I_2 chamber. Column chromatography separations were performed on silica gel 120 (ICN Chrom 32–63, 60 Å).

4.2 Synthesis of C_{60} adduct

2-(2-{2-[2-(Tetrahydropyran-2-yloxy)ethoxy]ethoxy}ethoxy)-ethanol (2). A solution of 3, 4-dihydro-2*H*-pyran (3.27 ml, 35.9 mmol) in dry DCM (50 ml) was added dropwise to a stirred, ice cold solution of tetraethylene glycol (**1**) (18.6 ml, 107.7 mmol) and *p*-toluenesulfonic acid monohydrate (0.137 g, 0.719 mmol) in dry DCM (500 ml) under a N_2 atmosphere. The solution was allowed to warm to room temperature and was stirred overnight. The DCM was removed *in vacuo* and the resulting oil purified by flash column chromatography (eluent; EtOAc–hexane–MeOH, 8 : 1 : 1). The solvent was removed *in vacuo* to afford a pale yellow oil (6.98 g, 71%). ν_{max}/cm^{-1} (film): 3491 m,br (O–H), 2940 m (C–H), 2871 m (C–H), 1119 m (THP, C–O–C), 1072 (C–O–C); δ_H (300 MHz; $CDCl_3$; Me_4Si) 4.57–4.60 (1 H, br, m, *THP*), 3.77–3.86 (2 H, br, m, *THP*), 3.42–3.51 (1 H, br, m, *THP*), 3.54–3.72 (15 H, br, m, HO($CH_2CH_2O)_3CH_2$–, *THP*), 2.82 (1 H, br, s, –*OH*), 1.45–1.85 (6 H, br, m, *THP*); δ_C (75 MHz; $CDCl_3$; Me_4Si) 98.8, 77.7, 73.1, 70.8, 70.7, 70.2, 66.9, 62.4, 61.8, 30.8, 30.7, 25.6, 19.7; *m*/*z* (ESMS): 301 ($[M + Na]^+$, 100%); *m*/*z* (HRMS): found 301.1617. Calc. mass for $C_{13}H_{26}O_6Na$: 301.1627.

Malonic acid bis-2-(2-{2-[2-(tetrahydropyran-2-yloxy)ethoxy]-ethoxy}ethoxy) ester (3). A solution of malonyl dichloride (0.70 ml, 7.19 mmol) in dry DCM (30 ml) was added dropwise to a stirred, ice cold solution of tetrahydropyranyl ether (**2**) (4.00 g, 14.40 mmol) and dry pyridine (1.45 ml, 18.00 mmol) in dry DCM (150 ml) under a N_2 atmosphere. The dark red coloured reaction mixture was allowed to warm to room temperature and stirred overnight. Followed by plug filtration (silica gel) washing first with DCM (200 ml) and secondly with EtOAc (300 ml) to elute the product. The EtOAc was removed *in vacuo* and the crude oil purified by flash chromatography (gradient elution: 70 to 100% EtOAc in hexane, increasing in increments of 5% EtOAc per 100 ml of eluent). The solvent was removed *in vacuo* to yield a yellow oil (2.24 g, 50%). δ_H (300 MHz; $CDCl_3$; Me_4Si) 4.58–4.63 (2 H, br, m, *THP*), 4.23–4.28 (4 H, br, m, 2(–$CH_2CH_2CO_2CH_2CH_2$)), 3.78–3.89 (4 H, br, m, *THP*), 3.54–3.71 (26 H, br, m, (–$CH_2O(CH_2CH_2O)_3$-CH_2O–), *THP*), 3.40–3.51 (4 H, br, m, –$O_2CCH_2CO_2$–, *THP*), 1.41–1.85 (12 H, br, m, *THP*), δ_C (75 MHz; $CDCl_3$; Me_4Si) 166.5, 99.9, 71.7, 69.9, 67.7, 65.6, 63.2, 42.3, 31.6, 26.5, 20.5; *m*/*z* (ESMS): 647 ($[M + Na]^+$, 100%); *m*/*z* (HRMS): calc. mass for $C_{29}H_{52}O_{14}Na$ 647.3255, found 647.3245.

3′*H*-Cyclopropa[1,9][5,6]fullerene-C_{60}-I_h-3,3′-carboxylic-2-(2-{2-[2-(tetrahydropyran-2-yloxy)ethoxy]ethoxy}ethoxy) ester (4).

A solution of 1,8-diazabicyclo(5.4.0)undec-7-ene (64 mg, 62.55 μmol) in dry PhMe (50 ml) was added dropwise to a stirred, ice cold solution of C_{60} (300 mg, 417 μmol), iodine (53 mg, 209 μmol) and bis-tetramalonate ester (**3**) (130 mg, 208 μmol) in dry PhMe (100 ml). The reaction was covered with aluminium foil and stirred overnight at room temperature under a N_2 atmosphere. Followed by plug filtration (silica gel) washing first with PhMe (200 ml) to remove the excess C_{60} and secondly with 5% MeOH in DCM (200 ml) to elute the product. The solvent was removed from the second fraction *in vacuo* and purified by flash chromatography (gradient elution: 0 to 3% MeOH in DCM; increasing in increments of 0.5% MeOH per 100 ml of eluent). The solvent was removed to yield a dark brown tar (140 mg, 49%). ν_{max}/cm^{-1} (nujol): 2939 m (C–H), 2871s (C–H), 1119s (THP, C–O–C), 1072s (C–O–C); δ_H (300 MHz; $CDCl_3$; Me_4Si) 4.58–4.63 (6 H, br, m, (–$CH_2CO_2CH_2CO_2CH_2$–), *THP*) 3.53–3.88 (30 H, br, m, 2(–$CH_2O(CH_2CH_2O)_3CH_2O$–) + *THP*), 3.42–3.51 (2 H, br, m, *THP*), 1.42–1.84 (12 H, br, m, *THP*); δ_C (75 MHz; $CDCl_3$; Me_4Si) 163.5, 145.2, 145.1, 144.8, 143.1, 143.0, 142.9, 142.2, 141.8, 140.9, 139.0, 98.9, 70.6, 70.5, 68.7, 66.6, 62.2, 30.5, 25.4, 19.5; *m*/*z* (MALDI-TOF MS): 1368 ([M + 2H]$^+$, 35%).

***H*-Cyclopropa[1,9][5,6]fullerene-C_{60}-I_h-3,3′-carboxylic-2-(2-{2-[2-(tetrahydropyran-2-yloxy)ethoxy]ethoxy}ethoxy)alcohol (C_{60} adduct).** TFAA (113 mg, 538 μmol) was added dropwise at room temperature to a solution of **4** (75 mg, 55 μmol) in a 1 : 1 mixture of DCM–MeOH (7 ml) followed by heating the reaction mixture at 50 °C for 2 h. The reaction mixture was allowed to cool to room temperature and the solvent was removed *in vacuo*. The crude solid was purified by flash chromatography (gradient elution: 0 to 2% MeOH in DCM, increasing in increments of 0.5% per 100 ml of eluent) and solvent removed *in vacuo* to yield a brown solid (53 mg, 82%). HPLC run in 50% MeCN and 50% H_2O showed compound was 97% pure (retention time: 13 min). Elemental analysis found: C, 80.51%; H, 2.84%. Calc. for $C_{79}H_{34}O_{12}$: C, 80.75%; H, 2.92%; ν_{max}/cm^{-1} (DCM) 3458 m (O–H), 3054 m (C–H), 2923 m (C–H), 1746s (C=O), 1072s (C–O–C); δ_H (300 MHz; $CDCl_3$; Me_4Si) 4.67–4.63 (4 H, br, m, (–$CH_2CO_2CCO_2CH_2$–)), 4.23–4.28 (4 H, br, m, 2(–$CO_2CH_2CH_2$)), 3.53–3.88 (24 H, br, m, 2(–$CH_2O(CH_2CH_2O)_3CH_2O$–); δ_C (75 MHz; $CDCl_3$; Me_4Si) 163.5, 147.0, 146.9, 146.4, 146.3, 145.6, 144.8, 144.7, 143.9, 143.6, 142.7, 140.8, 75.2, 75.2, 73.3, 73.0, 71.5, 69.0, 64.4; *m*/*z* (ESMS): 1197 ([M + Na]$^+$, 100%); *m*/*z* (HRMS): found 1197.1967. Calc. mass for $C_{79}H_{34}O_{12}Na$: 1197.1948.

4.3 Compound characterisation

4.3.1 NMR. ^{1}H nuclear magnetic resonance (NMR) spectra were recorded on a Bruker AC 300 (300.13 MHz) spectrometer. ^{13}C NMR spectra were recorded on a Bruker AV 300 (75.5 MHz) using Pendant pulse sequences. All chemical shifts are quoted in ppm to higher frequency from Me_4Si using deuterated chloroform ($CDCl_3$) as the lock and the residual solvent as the internal standard. The coupling constants are expressed in Hertz (Hz) with multiplicities abbreviated as follows; s = singlet, d = doublet, dd = double doublet, t = triplet, q = quartet and m = multiplet.

4.3.2 Mass spectrometry (MS). Electron impact mass spectroscopy (EIMS) was performed on VG Prospec. Low and high resolution electrospray mass spectrometry was performed on a micromass time of flight (TOF) instrument using methanol as the mobile phase. The matrix assisted laser desorption ionization–time of flight mass spectroscopy (MALDI–TOF MS) was performed on a Bruker Biflex. The samples were prepared by mixing the dissolved compounds with a matrix (sinapinic acid) and then allowing the solvent to evaporate to leave crystals as the samples.

4.3.3 Infrared spectroscopy (IR). The IR spectra were recorded as thin solid films on NaCl discs or KBr discs using a Perkin Elmer 1600 FT-IR. The solids were mixed with nujol to form a paste that was spread between the NaCl discs to form a thin film.

4.3.4 Elemental analysis. Elemental analysis was carried out on a Carlo Erba EA 1110 (C H N) instrument.

4.3.5 High performance liquid chromatography (HPLC). HPLC were recorded on a Dionex Summit System with Chromeleon Software, using a Summit UVD 170s UV/vis multi-channel detector with analytical flow cell. The analytical HPLC runs were performed on a Luna (Phenomenex), C_{18}, 250 × 4.6 mm ID, with 10 μm pore size column using a gradient of MeCN–H_2O.

4.4 Surface pressure-area (*Π–A*) isotherm studies

The *Π–A* isotherm studies were performed using a Nima 611 trough with Wilhelmy type balance. Prior to use, the trough was cleaned with $CHCl_3$, IPA and 3 times with 15 MΩ H_2O. The subphase used to form the Langmuir film was 15 MΩ H_2O. The C_{60} adduct (2.4 mg) was dissolved in $CHCl_3$ (5 ml) and 50 μl of the prepared solution was spread over the H_2O subphase at room temperature. The $CHCl_3$ was allowed to evaporate for 10 min before the isotherm studies were performed. The surface pressure was increased by reducing the surface area *via* controlling the closure of the barrier at a rate of 10 cm^2 min^{-1} from 200 to 20 cm^2 during the isotherm studies.

4.5 Preparation of the C_{60} adduct Langmuir films

The Langmuir films were prepared using a Nima 611 trough. Prior to the use, the trough was cleaned with $CHCl_3$, IPA and 3 times with 15 MΩ H_2O. The solution of the C_{60} adduct (50 μL, 0.41 mM) in $CHCl_3$ was spread over the H_2O subphase, left for 10 min for the solvent to evaporate and compressed at a rate of 10 cm^2 min^{-1}.

4.6 Preparation of the C_{60} adduct Langmuir–Blodgett film

The LB bilayer films were formed on hydrophobic Si/SiO_2 substrates. The substrates were cleaned prior to use by immersing in IPA, which was distilled before use. The Si/SiO_2 substrates were hydrophobised with hexamethyldisilazane by placing the substrates in a chamber containing hexamethyldisilazane ensuring that the meniscus of the silazane was just below the upper surface of the substrate. The substrates were left for 24 h in the chamber followed by sonication in $CHCl_3$, IPA and 15 MΩ

H_2O for 1 min each and dried with N_2 after each sonication. The hydrophobic Si/SiO_2 substrates were lowered into and raised from the Langmuir film (Π = 30 nN m^{-1}) at a velocity of 5 mm min^{-1} to afford the 2 or 3 bilayer LB films. Finally the LBFs were dried with N_2.

4.7 Photopatterning

Photopatterning was conducted using light from a frequency doubled argon ion laser (Coherent FreD 300C, Coherent U.K., Ely), which emits at 244 nm. For micrometre-scale patterning, a square grid mask consisting of 40 × 40 μm^2 square openings separated by 20 μm beams was positioned on the C_{60} adduct LBF and the sample was irradiated with power of 100 mW. The irradiation time was 1 min, and the area of illumination was typically 0.2–0.4 cm^2. The surface was then rinsed thoroughly with $CHCl_3$ and dried with N_2. For the scanning near-field photolithography, the laser was coupled to a Thermo-Microscopes Aurora III near-field scanning optical microscope fitted with a fused silica fiber probe (Veeco). The aperture diameter of the SNOM tip was ~70 nm. 16 lines were written for each probe velocity. The irradiated samples were rinsed thoroughly with $CHCl_3$ and dried with N_2.

5 Acknowledgements

JAP, DA and DT would like to thank the European Community (FP6, Contract No. NMP4-CT-2005-014006 NANO3D) and JAP would like to thank the Engineering and Physical Sciences Research Council (EPSRC, Adventurous Chemistry Scheme EP/C5238571) for financial support. GJL thanks RCUK (Grant EP/C523857/1), the RSC Analytical Chemistry Trust Fund and the EPSRC for their support.

6 References

1 A. K. Raub, A. Frauenglass, S. R. J. Brueck, W. Conley, R. Dammel, A. Romano, M. Sato and W. Hinsberg, *J. Vac. Sci. Technol.*, 2004, **B22**, 3459–3464.
2 M. Switkes and M. Rothschild, *J. Vac. Sci. Technol.*, 2001, **B19**, 2353–2356.
3 J. A. Hoffnagle, W. D. Hinsberg, M. Sanchez and F. A. Houle, *J. Vac. Sci. Technol.*, 1999, **B17**, 3306–3309.
4 D. B. Shao and S. C. Chen, *Nano Lett.*, 2006, **6**, 2279–2283.
5 W. L. Barnes, A. Dereux and T. W. Ebbesen, *Nature*, 2003, **424**, 824–830.
6 W. Srituravanich, N. Fang, C. Sun, Q. Luo and X. Zhang, *Nano Lett.*, 2004, **4**, 1085–1088.
7 A. Sundaramurthy, P. J. Schuck, N. R. Conley, D. P. Fromm, G. S. Kino and W. E. Moerner, *Nano Lett.*, 2006, **6**, 355–360; L. Wang, M. Ypuluri, E. X. Jin and X. Xu, *Nano Lett.*, 2006, **6**, 361–364.
8 S. Sun, K. S. L. Chong and G. J. Leggett, *J. Am. Chem. Soc.*, 2002, **124**, 2414–1415.
9 S. Sun and G. J. Leggett, *Nano Lett.*, 2002, **2**, 1223–1227.
10 S. Sun and G. J. Leggett, *Nano Lett.*, 2004, **4**, 1381–1384.
11 S. Sun, K. S. L. Chong and G. J. Leggett, *Nanotechnology*, 2005, **16**, 1798–1808.
12 R. E. Ducker and G. J. Leggett, *J. Am. Chem. Soc.*, 2006, **128**, 392–393.
13 S. Sun, M. Montague, K. Critchley, M.-S. Chen, W. J. Dressick, S. D. Evans and G. J. Leggett, *Nano Lett.*, 2006, **6**, 29–33.
14 S. Sun, P. Mendes, K. Critchley, S. Diegoli, M. Hanwell, S. D. Evans, G. J. Leggett, J. A. Preece and T. H. Richardson, *Nano Lett.*, 2006, **6**, 345–350.
15 J.-F. Nierengarten, *New J. Chem.*, 2004, **28**, 1177–1191; D. Bonifazi, O. Enger and F. Diederich, *Chem. Soc. Rev.*, 2007, **36**, 390–414.
16 H. W. Kroto, J. R. Heath, S. C. O'Brien, R. F. Curl and R. E. Smalley, *Nature*, 1985, **318**, 162–163.
17 A. W. Jensen, S. R. Wilson and D. I. Schuster, *Bioorg. Med. Chem.*, 1996, **4**, 767–779; S. Bosi, T. D. Ros, G. Spattuto and M. Prato, *Eur. J. Med. Chem.*, 2003, **38**, 913–923; B. Belgorodsky, L. Fadeev, V. Ittah, H. Benyamini, S. Zeiner, D. Huppert, A. B. Kotlyar and M. Gozin, *Bioconjugate Chem.*, 2005, **16**, 1058–1062.
18 M. Prato, *J. Mater. Chem.*, 1997, **7**, 1097–1109; R. M. Metzger, J. W. Baldwin, W. J. Shumate, I. R. Peterson, P. Mani, G. J. Mankey, T. Morris, G. Szulczewski, S. Bosi, M. Prato, A. Comito and Y. Rubin, *J. Phys. Chem. B*, 2003, **107**, 1021–1027; M. E. Rincón, H. Hu, J. Campos and J. Ruiz-Garcia, *J. Phys. Chem. B*, 2003, **107**, 4111–4117; F. Deng, Y. Yang, S. Hwang, Y.-S. Shon and S. Chen, *Anal. Chem.*, 2004, **76**, 6102–6107; D. R. Talham, *Chem. Rev.*, 2004, **104**, 5479–5501; N. Martin, *Chem. Commun.*, 2006, 2093–2104.
19 F. Fungo, L. Otero, C. D. Borsarelli, E. N. Durantini, J. J. Silber and L. Sereno, *J. Phys. Chem. B*, 2002, **106**, 4070–4078; H. Imahori and S. Fukuzumi, *Adv. Funct. Mater.*, 2004, **14**, 525–536; T. M. Figueira-Duarte, A. Gégout and J.-F. Nierengarten, *Chem. Commun.*, 2007, 109–119.
20 A. M. Rao, P. Zhou, K.-A. Wang, G. T. Hager, J. M. Holden, Y. Wang, W.-T. Lee, X.-X. Bi, P. C. Eklund, D. S. Cornett, M. A. Duncan and I. J. Amster, *Science*, 1993, **259**, 955–957.
21 P. Zhou, Z.-H. Dong, A. M. Rao and P. C. Eklund, *Chem. Phys. Lett.*, 1993, **211**, 337–340.
22 M. Menon, K. R. Subbaswamy and M. Sawtarie, *Phys. Rev. B*, 1994, **49**, 13966–13969.
23 P. W. Stephens, G. Bortel, G. Faigel, M. Tegze, A. Jánossy, S. Pekker, G. Oszlanyl and L. Forró, *Nature*, 1994, **370**, 636–639; Y. Wang, J. M. Holden, A. M. Rao, P. C. Eklund, U. D. Venkateswaran, D. Eastwood and R. L. Lidberg, *Phys. Rev. B*, 1995, **51**, 4547–4556.
24 T. L. Makarova, *Semiconductors*, 2001, **35**, 243–278.
25 A. Hassanien, J. Gasperič, J. Demsar, I. Muševic and D. Mihailovic, *Appl. Phys. Lett.*, 1997, **70**, 417–419; É. Kováts, G. Oszlányl and S. Pekker, *J. Phys. Chem. B*, 2005, **109**, 11913–11917.
26 S. Ōsawa, M. Sakai and E. Ōsawa, *J. Phys. Chem. A*, 1997, **101**, 1378–1383; D. Porezag, M. R. Pederson, T. Frauenheim and T. Köhler, *Phys. Rev. B*, 1995, **52**, 14963–14970; G. E. Scuseria, *Chem. Phys. Lett.*, 1996, **257**, 583–586; M. Suzuki, T. Iida and K. Nasu, *Phys. Rev. B*, 2000, **61**, 2188–2198.
27 S. G. Stepanian, V. A. Karachevtsev, A. M. Plokhotnichenko, L. Adamowicz and A. M. Rao, *J. Phys. Chem. B*, 2006, **110**, 15769–15775.
28 A. P. G. Robinson, P. E. Palmer, T. Tada, T. Kanayama and J. A. Preece, *Appl. Phys. Lett.*, 1998, **72**, 1302–1304.
29 T. Tada, T. Kanayama, A. P. G. Robinson, R. E. Palmer and J. A. Preece, *J. Photopolym. Sci. Technol.*, 1998, **11**, 581–584.
30 A. P. G. Robinson, P. E. Palmer, T. Tada, T. Kanayama, J. A. Preece, D. Philip, U. Jonas and F. Diederich, *Chem. Phys. Lett.*, 1998, **289**, 586–580.
31 A. P. G. Robinson, R. E. Palmer, T. Tada, T. Kanayama, E. J. Shelley and J. A. Preece, *Mater. Res. Symp. Proc.*, 1999, **546**, 219–224.
32 A. P. G. Robinson, R. E. Palmer, T. Tada, T. Kanayama, E. J. Shelley and J. A. Preece, *Chem. Phys. Lett.*, 1999, **312**, 469–474.
33 J.-F. Nierengarten, V. Gramlich, F. Cardullo and F. Diederich, *Angew. Chem., Int. Ed. Engl.*, 1996, **35**, 2101–2103; J.-F. Nierengarten, A. Herrman, R. R. Tykwinski, M. Rűttimann and F. Diederich, *Helv. Chim. Acta*, 1997, **80**, 293–316; E. J. Shelley, *PhD thesis*, University of Birmingham, 2002, p. 108.
34 E. Vuorimaa, T. Vuorinen, N. Tkachenko, O. Cramariuc, T. Hukka, S. Nummelin, A. Shivanyuk, K. Rissanen and H. Lemmetyinen, *Langmuir*, 2001, **17**, 7327–7331.
35 J.-L. Gallani, D. Felder, D. Guillon, B. Heinrich and J.-F. Nierengarten, *Langmuir*, 2002, **18**, 2908–2913.
36 Y. Gao, Z. Tang, E. Watkins, J. Majewski and H.-L. Wang, *Langmuir*, 2005, **21**, 1416–1423.